Time-delayed Raman-enhanced nondegenerate four-wave mixing with a broadband laser source

Xin Mi, Zuhe Yu, Qian Jiang, and Panming Fu
Institute of Physics, Chinese Academy of Sciences, P.O. Box 603, Beijing 100 080, China
(Received 10 February 1993)

We report an experiment of the time-delayed Raman-enhanced nondegenerate four-wave mixing (RENFWM) with a broadband laser in carbon disulfide (CS_2). We studied the RENFWM signal intensity as a function of the relative time delay τ between two beams which originate from a single broadband laser source. Our results indicate that the temporal behavior of the RENFWM is asymmetric with the maximum of the signal shifted from $\tau=0$. Furthermore, unlike the corresponding coherent Stokes Raman scattering (CSRS) no coherent spike appears at $\tau=0$. From our experimental results the relaxation time of the Raman mode can be extracted directly. We present a second-order coherence function theory to elucidate the physics of the basic features of the time-delayed RENFWM. We also discuss the difference between the RENFWM and the CSRS from a physical viewpoint.

PACS number(s): 42.65.Dr, 42.65.Hw

I. INTRODUCTION

Much attention has been paid to the study of various ultrafast phenomena by using incoherent light for the past decade. Morita and Yajima [1] first suggested theoretically that in a two-level system the time-delayed four-wave mixing (FWM) with incoherent light can be used to measure the dephasing time of the system. The time resolution of this method is determined by the correlation time τ_c of the light source. For an incoherent light with a wide spectral width, τ_c is much shorter than its temporal duration, therefore subpicosecond dephasing time can be measured even with a cw light source. This principle was verified in an experiment performed by Asaka *et al.* [2]. They studied the $^4I_{9/2}\leftrightarrow{}^2G_{7/2},{}^4G_{5/2}$ transition of Nd^{3+} doped in silicate glass using a cw dye laser source with spectral width 1.4 nm. The transverse relaxation time T_2 was measured to be 57 psec, which is consistent with the result obtained from an accumulated photon echo experiment. The same transition has also been studied by using nanosecond laser pulses [3]. On the other hand, Beach, DeBeer, and Hartmann [4] performed a time-delayed FWM with incoherent light on the $3S$ to $3P$ transition in Na. They observed a large-scale 1.9-psec modulation which is associated with the fine structure of the $3P$ state. A new type of the pump-probe technique with incoherent light has also been proposed to measure the longitudinal relaxation time T_1 of a system [5].

Hattori, Terasaki, and Kobayashi [6] have applied the principle that the correlation time determines the resolution time to the transient coherent Raman spectroscopy. Specifically, they performed the coherent Stokes Raman scattering (CSRS) with three beams. Two of them are incoherent light originating from a single source, while the third beam is coherent with frequency higher than the incoherent light by a vibrational energy of the Raman active mode. In this experiment, the relative time delay between two incoherent light beams is variable. They studied the time-delayed dependence of the CSRS signal intensity and found that it offered the information about the dephasing time of the Raman vibrational mode with a resolution time determined only by the correlation time of the incoherent light.

Recently, we have made a systematic study of the effect of laser coherence on time-delayed Raman-enhanced nondegenerate four-wave mixing (RENFWM) [7]. It is found that RENFWM spectrum depends on the relative time delay between two incident beams which originate from a single laser source. In the case that a thermal effect exists in the sample, the thermal background may be eliminated completely when the relative time delay is much longer than the laser correlation time [7,8]. We also study the time-delayed dependence of the RENFWM signal intensity when the frequencies of the incident beams are fixed. The most interesting thing occurs for the case that the laser source has very short correlation time τ_c. When $\gamma_R\tau_c \ll 1$, the RENFWM signal decays with decay rate $2\gamma_R$ at the tail of the signal, hence the dephasing time of the vibrational mode can be deduced. Here, γ_R is the dephasing rate of the Raman mode. Although physically the time-delayed RENFWM with incoherent light is similar to the corresponding CSRS [6], there are some important differences between them. First, the temporal behavior of the RENFWM is asymmetric with the maximum of the signal shifted from zero time delay. Furthermore, in the CSRS there is a coherence spike which is related to the autocorrelation function of the incoherent light beams. In contrast, the coherence spike is absent in the RENFWM. In this paper, we report an experiment of the time-delayed RENFWM with broadband laser sources. We also present a second-order coherence function theory, which provides a deeper insight into the physics of the time-delayed RENFWM.

The paper is organized as follows. In Sec. II the experimental setup and the results of the time-delayed RENFWM with broadband laser source are presented. In Sec. III we develop a second-order coherence function theory to elucidate the underlying mechanism of the time-delayed RENFWM. Section IV is the discussion and conclusion. The difference between RENFWM and

CSRS from a physical viewpoint has been discussed in this section.

II. EXPERIMENT

RENFWM is a third-order nonlinear phenomenon with three incident beams involved [9,10]. The basic geometry is shown in Fig. 1. Beams 1 and 2 have the same frequency ω_1 and a small angle exists between them. Beam 3 with frequency ω_3 is almost propagating along the opposite direction of beam 1. In a Kerr medium, the nonlinear interaction of beams 1 and 2 with the medium gives rise to a molecular-reorientational grating. The FWM signal is the result of the diffraction of beam 3 by the grating. Now, if $|\omega_1-\omega_3|$ is near the Raman resonant frequency ω_R, a moving grating formed by the interference of beams 2 and 3 will excite the Raman-active vibrational mode of the medium and enhance the FWM signal. The FWM signal (beam 4) has frequency ω_3 and is propagating along the opposite direction of beam 2 approximately. In these experiments, we are interested in the dependence of the FWM signal intensity on the relative time delay between beams 1 and 2, which are broadband light beams originating from a single laser source.

The experimental setup is shown in Fig. 2. We studied the 655.7-cm^{-1} vibrational mode of carbon disulfide (CS_2), which was contained in a sample cell with thickness 10 mm. The second harmonic of a Quanta-Ray YAG laser (where YAG denotes yttrium aluminum garnet) as used to pump two dye lasers (D1 and D2). To obtain broadband light source, the cavity of D1 is made with a 1200-line/mm grating and an output mirror only with no optical component to expand the beam diameter. The laser has wavelength 589.2 nm, linewidth 0.1 nm, output energy 1.5 mJ, and pulse width 5 nsec. The laser output was split into beam 1 and beam 2 after passing through a beam splitter (BS1), and the two beams intersect in the sample with a small angle (1.3°) between them. Two Soleil-Babinet compensators (CP1 and CP2) were employed to set up the desired polarization of these beams. The relative time delay between beams 1 and 2 could be varied by an optical delay line controlled by a stepping motor. Beam 3, originating from a narrowband dye laser D2, has linewidth 0.01 nm, output energy 1 mJ, and pulse width 5 nsec. The wavelength of beam 3 could be scanned by a computer-controlled stepping motor. It was set to approximately 567.3 nm so that the 655.7-cm^{-1} Raman active mode of CS_2 could be excited. All the incident beams were focused to spots with diameters of approximately 0.5 mm. After passing through a polarizer, the RENFWM signal was detected by a photodiode and then fed into an EG&G 4203 signal averager for data averaging. A computer was used for data processing and for controlling the stepping motor to vary the relative time delay or the wavelength of beam 3.

FIG. 1. Schematic diagram of the geometry of Raman-enhanced nondegenerate four-wave mixing.

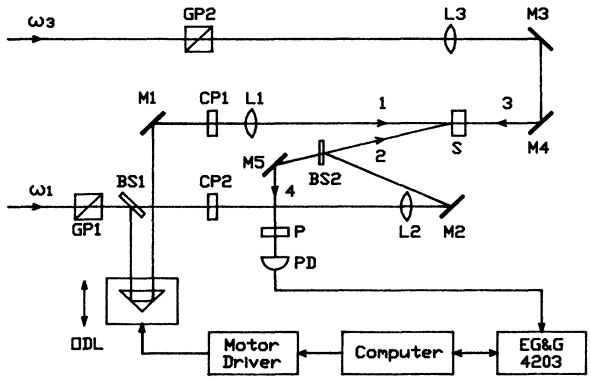

FIG. 2. Experimental setup. BS's, beam splitters; M's, mirrors; L's, lenses; GP's, Glan prisms; CP's, Soleil-Babinet compensators; P, polarizer; PD, photodiode; ODL, optical delay line; S, sample.

We first studied the RENFWM spectrum at $\tau=0$ by scanning the frequency of beam 3. Here τ is the time delay of beam 1 with respect to beam 2. The polarization configuration is the following: $\mathcal{E}^{(1)}\|\mathcal{E}^{(2)}\|(1/\sqrt{2})(\mathbf{x}+i\mathbf{y})$, $\mathcal{E}^{(3)}\|\mathbf{x}$, and $\mathcal{E}^{(4)}\|\mathbf{y}$, where $\mathcal{E}^{(i)}$ is the polarization of the ith beam. Due to the Kleinman symmetry the nonresonant background from the molecular reorientation can be suppressed greatly, therefore the RENFWM spectrum has symmetrical line shape [10]. Our results are shown in Fig. 3. Theoretically, the dependence of the RENFWM signal intensity on the frequency detuning can be derived from Eq. (7) or (8) in Ref. [7]. Considering the Raman terms only, we have at $\tau=0$ the RENFWM signal intensity

$$I(\Delta)\propto\frac{(\gamma_R+\alpha+\alpha_3)}{(\gamma_R+\alpha+\alpha_3)^2+\Delta^2}\ . \tag{1}$$

Here the frequency detuning $\Delta=(\omega_3-\omega_1)-\omega_R$, $\alpha=\delta\omega_1/2$, and $\alpha_3=\delta\omega_3/2$ with $\delta\omega_1$ and $\delta\omega_3$ the laser linewidth (full width at half maximum) of beams 1 and 3, respectively. The solid curve in the figure is the theoretical curve. In this calculation, the relaxation rate $\gamma_R=5.0\times10^{10}$ sec^{-1} [11], while $\alpha_3=2.9\times10^{10}$ sec^{-1}

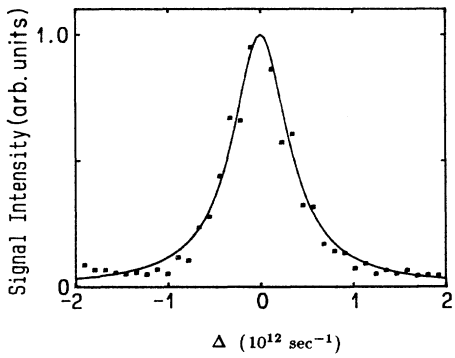

FIG. 3. RENFWM spectrum at $\tau=0$ for the polarization configuration: $\mathcal{E}^{(1)}\|\mathcal{E}^{(2)}\|(1/\sqrt{2})(\mathbf{x}+i\mathbf{y})$, $\mathcal{E}^{(3)}\|\mathbf{x}$, and $\mathcal{E}^{(4)}\|\mathbf{y}$. Solid curve: theoretical curve with $\gamma_R=5.0\times10^{10}$ sec^{-1}, $\alpha_3=2.9\times10^{10}$ sec^{-1}, and $\alpha=2.79\times10^{11}$ sec^{-1}.

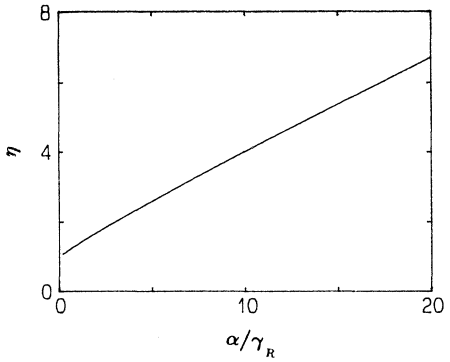

FIG. 4. Theoretical curve of η vs α/γ_R for $\Delta=0$ and $\alpha_3=0$.

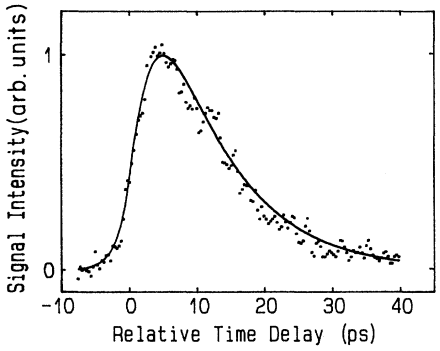

FIG. 5. The RENFWM signal intensity as a function of the relative time delay between beams 1 and 2 at exact resonance ($\Delta=0$) for the following polarization configuration: $\mathcal{E}^{(1)}\|\mathcal{E}^{(2)}\|(1/\sqrt{2})(\mathbf{x}+i\mathbf{y})$, $\mathcal{E}^{(3)}\|\mathbf{x}$, and $\mathcal{E}^{(4)}\|\mathbf{y}$. The τ-independent background has been subtracted in the figure. Solid curve: theoretical curve with $\gamma_R=5.0\times10^{10}$ sec^{-1}, $\alpha_3=2.9\times10^{10}$ sec^{-1}, and $\alpha=2.79\times10^{11}$ sec^{-1}.

corresponding to the 0.01-nm laser linewidth of beam 3. Through the fit of the experimental data, we obtain $\alpha=2.79\times10^{11}$ sec^{-1}. It should be noted that, although there is uncertainty on the value of α_3, it will not affect the fitting value of α too much because $\alpha\gg\alpha_3$.

We then studied the RENFWM signal intensity as a function of the relative time delay between beams 1 and 2 when the frequencies of the incident beams are fixed. Since the RENFWM with broadband laser source is closely related to the corresponding CSRS, which has been used to measure the ultrafast vibrational dephasing of the Raman mode, here we restrict ourselves to the Raman terms and neglect the contribution from the molecular-reorientational grating. Now, as in the case of CSRS, in RENFWM the τ-dependent signal is accompanied by a constant background [7]. Let I_S be the maximum intensity of the τ-dependent signal and I_B the intensity of the background. We define $\eta=I_B/I_S$ as the ratio between I_B and I_S. Figure 4 presents the theoretical curve of η versus α/γ_R for $\Delta=0$ and $\alpha_3=0$. In the limit of $\alpha\gg\gamma_R$, I_B is larger than I_S by a factor of approximately $\alpha/4\gamma_R$. In order to observe the τ dependence of the RENFWM signal, the signal-to-noise ratio of the experiment should be larger than η. In this experiment, we have $\eta\simeq2.8$, corresponding to $\alpha/\gamma_R\simeq5.6$, while the signal-to-noise ratio is about 10.

To eliminate the contribution from the molecular-reorientational grating, we employed the following polarization configuration again: $\mathcal{E}^{(1)}\|\mathcal{E}^{(2)}\|(1/\sqrt{2})(\mathbf{x}+i\mathbf{y})$, $\mathcal{E}^{(3)}\|\mathbf{x}$, and $\mathcal{E}^{(4)}\|\mathbf{y}$. Further, the wavelength of beam 3 was set to 567.3 nm, so that the 655.7-cm^{-1} mode of CS_2 could be excited exactly at resonance. Figure 5 presents the results where each data point was an average of 60 laser shots and then the whole data set was smoothed. The τ-independent background has been subtracted in the figure. Our results exhibit all the basic features of the time-delayed RENFWM predicted by the theory. First, RENFWM is asymmetric with the maximum of the RENFWM signal shifted from $\tau=0$. Furthermore, unlike the corresponding CSRS no coherent spike appears at $\tau=0$.

We analyzed our experimental results by the theory presented in Ref. [7]. Considering the Raman terms only, we have from Eqs. (7) and (8) of Ref. [7] the τ-dependent parts of the RENFWM signal at $\Delta=0$ for (i) $\tau>0$,

$$
\begin{aligned}
I(\tau)\propto&\exp(-2\alpha|\tau|)\left[\frac{1}{(\gamma_R-\alpha)(\gamma_R-\alpha+\alpha_3)}\right]\\
&+\exp(-2\gamma_R|\tau|)\left[\frac{1}{(\gamma_R-\alpha)(\gamma_R-\alpha-\alpha_3)}+\frac{1}{(\gamma_R+\alpha)(\gamma_R+\alpha+\alpha_3)}-\frac{2}{(\gamma_R+\alpha+\alpha_3)(\gamma_R-\alpha-\alpha_3)}\right]\\
&-4\exp[-(\gamma_R+\alpha+\alpha_3)|\tau|]\left[\frac{\alpha}{(\gamma_R-\alpha-\alpha_3)(\gamma_R-\alpha+\alpha_3)(\gamma_R+\alpha+\alpha_3)}\right],
\end{aligned}
\tag{2}
$$

and (ii) $\tau<0$,

$$
I(\tau)\propto\exp(-2\alpha|\tau|)\left[\frac{1}{(\gamma_R+\alpha)(\gamma_R+\alpha+\alpha_3)}\right]. \tag{3}
$$

The solid curve in Fig. 5 is the theoretical curve, in which the same set of parameters used in the calculation of the RENFWM spectrum (Fig. 3) has been employed, i.e., $\gamma_R=5.0\times10^{10}$ sec^{-1}, $\alpha_3=2.9\times10^{10}$ sec^{-1}, and $\alpha=2.79\times10^{11}$ sec^{-1}. The agreement between the experiment and the theory is quite good.

III. SECOND-ORDER COHERENCE FUNCTION THEORY OF TIME-DELAYED RAMAN-ENHANCED NONDEGENERATE FOUR-WAVE MIXING

We have developed a fourth-order coherence function theory to study the effect of laser coherence on RENFWM in Ref. [7]. In order to gain further insight into the underlying mechanism of the time-delayed RENFWM, here we develop a second-order coherence function theory. This theory is valid when we are only interested in the τ-dependent part of the RENFWM signal. Furthermore, beams 1 and 2 are multimode thermal sources and beam 3 has much narrower linewidth so that it can be considered as a coherent light.

The complex incident laser fields can be written as

$$E_i(\mathbf{r},t)=A_i(\mathbf{r},t)\exp(-i\omega_i t) =\epsilon_i u_i(t)\exp[i(\mathbf{k}_i\cdot\mathbf{r}-\omega_i t)] \quad (i=1,2,3) \tag{4}$$

where $A_i(\mathbf{r},t)=\epsilon_i u_i(t)\exp(i\mathbf{k}_i\cdot\mathbf{r})$. ϵ_i and $\mathbf{k}_i$ are the constant field magnitude and the wave vector of the ith beam, respectively. $u_i(t)$ is a dimensionless statistical factor that contains the phase and the amplitude fluctuations. Since beams 1 and 2 come from a single laser source with time delay between them, we have $u_1(t)=u(t-\tau), u_2(t)=u(t)$. On the other hand, we have $u_3(t)=1$ because beam 3 is assumed to be a coherent light.

We assume that ω_1 and ω_3 are far off resonance with electronic transitions. At exact Raman resonance the normal coordinate $Q_R(\mathbf{r},t)$ induced by the beat between beams 2 and 3 satisfies [12]

$$\frac{\partial Q_R}{\partial t}+\gamma_R Q_R=\frac{i\alpha_R}{4\hbar}A_2^* A_3 . \tag{5}$$

Here α_R is a parameter denoting the strength of the Raman interaction. The formal solution of Eq. (5) is

$$Q_R(\mathbf{r},t)=\frac{i\alpha_R}{4\hbar}\int_0^\infty dt' A_2^*(\mathbf{r},t-t') \times A_3(\mathbf{r},t-t')\exp(-\gamma_R t') . \tag{6}$$

We have the nonlinear polarization responsible for the Raman-enhanced FWM signal

$$\begin{aligned}P(\mathbf{r},t)&=\tfrac{1}{2}N\alpha_R Q_R(\mathbf{r},t)E_1(\mathbf{r},t)\exp[i(\omega_1-\omega_3)t]\\&=i(\chi_R\gamma_R)\epsilon_1\epsilon_2^*\epsilon_3\exp i[(\mathbf{k}_1-\mathbf{k}_2+\mathbf{k}_3)\cdot\mathbf{r}-\omega_3 t]\int_0^\infty dt' u_1(t)u_2^*(t-t')\exp(-\gamma_R t')\\&=i(\chi_R\gamma_R)\epsilon_1\epsilon_2^*\epsilon_3\exp i[(\mathbf{k}_1-\mathbf{k}_2+\mathbf{k}_3)\cdot\mathbf{r}-\omega_3 t]\int_0^\infty dt' u(t-\tau)u^*(t-t')\exp(-\gamma_R t') ,\end{aligned} \tag{7}$$

with $\chi_R=N\alpha_R^2/8\hbar\gamma_R$ and N the density of molecules.

The FWM signal is proportional to the average of the absolute square of $P(\mathbf{r},t)$ over the random variable of the stochastic process $\langle|P(\mathbf{r},t)|^2\rangle$, which involves fourth-order coherence function of $u(t)$. We assume that beam 1 (beam 2) is a multimode thermal source. In the case that we are only interested in the τ-dependent part of the signal, the FWM signal intensity can be well approximated by the absolute square of the stochastic average of the polarization $|\langle P(\mathbf{r},t)\rangle|^2$ [13]. $\langle P(\mathbf{r},t)\rangle$ involves second-order coherence function of $u(t)$. Assuming that beam 1 (beam 2) has Lorentzian line shape, then we have

$$\langle u(t)u^*(t-\tau)\rangle=\exp(-\alpha|\tau|) ; \tag{8}$$

therefore

$$\langle P(\mathbf{r},t)\rangle=i(\chi_R\gamma_R)\epsilon_1\epsilon_2^*\epsilon_3 \times\exp i[(\mathbf{k}_1-\mathbf{k}_2+\mathbf{k}_3)\cdot\mathbf{r}-\omega_3 t] \times\int_0^\infty dt'\exp(-\alpha|t'-\tau|)\exp(-\gamma_R t') . \tag{9}$$

After performing the integral in Eq. (9), we obtain, for (i) $\tau>0$,

$$\langle P(\mathbf{r},t)\rangle=i\left[\frac{\chi_R\gamma_R}{\gamma_R-\alpha}\right]\epsilon_1\epsilon_2^*\epsilon_3\exp i[(\mathbf{k}_1-\mathbf{k}_2+\mathbf{k}_3)\cdot\mathbf{r}-\omega_3 t] \times\left[\exp(-\alpha|\tau|)-\frac{2\alpha}{\gamma_R+\alpha}\exp(-\gamma_R|\tau|)\right] , \tag{10}$$

and (ii) $\tau<0$,

$$\langle P(\mathbf{r},t)\rangle=i\left[\frac{\chi_R\gamma_R}{\gamma_R+\alpha}\right]\epsilon_1\epsilon_2^*\epsilon_3\exp i[(\mathbf{k}_1-\mathbf{k}_2+\mathbf{k}_3)\cdot\mathbf{r}-\omega_3 t] \times\exp(-\alpha|\tau|) . \tag{11}$$

It can be shown easily that the RENFWM signal intensity deduced from Eqs. (10) and (11) by taking the absolute square of $\langle P(\mathbf{r},t)\rangle$ is consistent with Eqs. (2) and (3) if we set $\alpha_3=0$.

From the second-order coherence function theory, the stochastic average of the nonlinear polarization determines the basic features of the temporal behavior of the RENFWM. As discussed before, the establishment of the nonlinear polarization consists of two steps. First, normal parameter Q_R is induced through the nonlinear interaction between the medium and two incident beams. Since Q_R satisfies the first-order differential equation, the integration effect is involved in this process [see Eq. (6)]. The induced normal parameters Q_R is then probed by another incident beam, which leads to the generation of the nonlinear polarization. In the case that ω_1 is far off resonance with electronic transitions, this step is an instantaneous process and the polarization is proportional to the direct production of the normal parameter and the probe beam field [see Eq. (7)]. For the Raman-active mode, the normal parameter Q_R is induced by beam 2 and a coherent light beam 3. Due to the integration effect, Q_R at time t is the summation of the normal pa-

rameter induced at time before t. Since the Raman-active mode decays with rate γ_R, we have a weight factor $\exp(-\gamma_R t')$ in Eq. (6). Q_R is probed by beam 1 at time t instantaneously. If beam 1 is delay with respect to beam 2 by τ, then only that part of the normal parameter induced at time approximately τ before are correlated with the probe beam. The factor $\exp(-\alpha|t'-\tau|)$ in Eq. (9) reflects this mutual correlation between the normal parameter and the probe beam.

The temporal behavior of the time-delayed RENFWM can be understood from Eq. (9) directly. Figure 6 shows functions $\exp(-\gamma_R t')$ and $\exp(-\alpha|t'-\tau|)$, where $\exp(-\gamma_R t')$ describes the decay of the Raman mode, while $\exp(-\alpha|t'-\tau|)$ gives the mutual correlation between the Raman mode and the probe beam. Due to the integration effect, the nonlinear polarization is proportional to the integral over t' (from 0 to ∞) of the production of these two functions. Now, we discuss the relative time delay when the maximum of the RENFWM signal intensity occurs. The function $\exp(-\alpha|t'-\tau|)$ can be divided into two parts: region I for $t'<\tau$ and region II for $t'>\tau$. When $\tau=0$, only region II has contribution to the integral. However, region I gives additional contributions to the integral when $\tau>0$. Therefore, the delay time such that RENFWM signal intensity is maximum $\tau_{\max}$ should not occur at 0, but shift to $\tau_{\max}>0$. Next, we consider the τ dependence of the RENFWM signal when $\alpha\gg\gamma_R$ and $\tau>0$. In this case, the function $\exp(-\alpha|t'-\tau|)$ is so sharp at $t'=\tau$ that it provides an extremely good temporal resolution and $\langle P(\mathbf{r},t)\rangle$ decays with rate γ_R. More specifically, we can approximate $\exp(-\alpha|t'-\tau|)$ by a δ function, i.e.,

$$\exp(-\alpha|t'-\tau|)\simeq\frac{2}{\alpha}\delta(t'-\tau)\ . \tag{12}$$

Substituting Eq. (12) into Eq. (9), we have

$$\langle P(\mathbf{r},t)\rangle=\epsilon_1\epsilon_2^*\epsilon_3\exp i[(\mathbf{k}_1-\mathbf{k}_2+\mathbf{k}_3)\cdot\mathbf{r}-\omega_3 t]\times\left[i\frac{2\chi_R\gamma_R}{\alpha}\exp(-\gamma_R\tau)\right]\ . \tag{13}$$

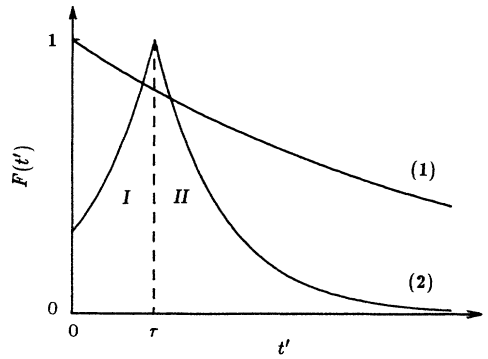

FIG. 6. Schematic to describe the second-order coherence function theory of the time-delayed RENFWM. $F(t')=\exp(-\gamma_R t')$ for curve (1) and $F(t')=\exp(-\alpha|t'-\tau|)$ for curve (2). The stochastic average of the nonlinear polarization $\langle P\rangle$ is proportional to the integral over t' (from 0 to ∞) of the production of these two functions.

The above equation indicates that the τ dependence of $\langle P(\mathbf{r},t)\rangle$ decays with rate γ_R as we predicted. We then consider the case that beam 2 is delayed from beam 1 (i.e., $\tau<0$). In this case, the integral in Eq. (9) involves only part of region II. Further, the area of region II involved in the integral decreases with decay rate α as the time delay increases, therefore the τ dependence of the RENFWM signal reflects the coherence time of the laser. Figure 6 can also be used to discuss the case when $\alpha\ll\gamma_R$. In this limit, $\exp(-\gamma_R t')$ decays so rapidly that the integral in Eq. (9) is determined by the function $\exp(-\alpha|t'-\tau|)$ at $t'=0$. In other words, $\langle P(\mathbf{r},t)\rangle$ decays with rate α when $|\tau|$ increases. Physically, the relaxation time of the Raman mode is so short that the Raman mode excited by beam 2 and beam 3 should be probed immediately by beam 1. Therefore, the temporal behavior of the RENFWM reflects the mutual correlation between beam 1 and beam 2. Finally, we note that according to the above discussion, no coherence spike exists at $\tau=0$, which is different drastically from the corresponding CSRS with incoherent light.

IV. DISCUSSION AND CONCLUSION

One of the most important application of the time-delayed RENFWM is to use it to measure the relaxation time of the Raman-active mode. From Eq. (2), we have that the RENFWM signal intensity decays exponentially with decay rate $2\gamma_R$ when $\alpha\gg\gamma_R$ and $\tau\gg\alpha^{-1}$. In order to employ this method to measure the relaxation time of the Raman mode, it is better to use laser with broader linewidth. However, as α/γ_R increases, the τ-independent background of the RENFWM signal increases also, which makes the study of the temporal behavior of RENFWM difficult. This problem is especially serious in the pulse experiments because the signal-to-noise ratio is usually poor. A similar problem exists also in the corresponding time-delayed CSRS. In our experiment, we have $\alpha/\gamma_R\simeq5.6$. Our question is that with this modest value of α/γ_R, how well is the temporal resolution? Can we obtain the information about the relaxation time of the Raman mode directly from the experimental results? To answer this, we replot the logarithm of the RENFWM signal intensity as a function of τ in Fig. 7. We also draw a straight line along the tail of

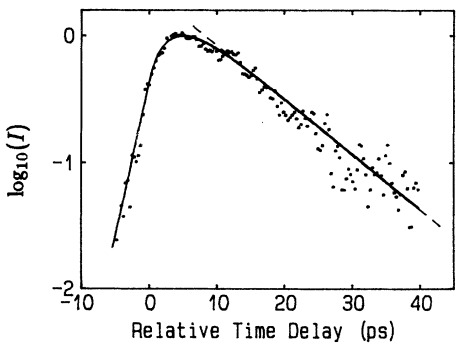

FIG. 7. The logarithm of the RENFWM signal intensity vs τ. The dashed line is a straight line along the tail of the theoretical curve.

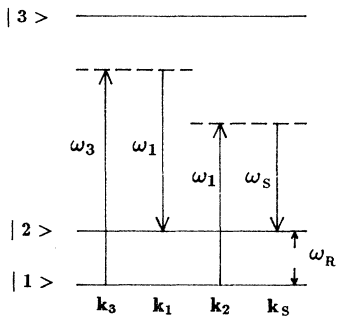

FIG. 8. Schematic of the CSRS with incoherent light. $\mathbf{k}_1$ and $\mathbf{k}_2$ are interchangeable in the figure.

the theoretical curve. It shows that the logarithm of the RENFWM signal intensity versus τ is basically a straight line when $\tau > 10$ psec; therefore the relaxation rate of the Raman mode can be deduced directly from the slope of this line. Actually, we have fitted the tail of the signal ($\tau > 10$ psec) by a least squares fit program and obtained the relaxation time 10.5 psec, which is consistent with the value of 10 psec measured by a method of time-resolved stimulated Raman gain [11]. In other words, it is possible to measure the relaxation time of the Raman-active mode by the time-delayed RENFWM even when the value of α/γ_R is not too large.

Now, we discuss the difference between RENFWM and CSRS from a physical viewpoint. Figure 8 shows the basic principle of CSRS. Two vibrational levels $|1\rangle$ and $|2\rangle$ belong to the ground electronic state, whereas $|3\rangle$ belongs to the excited electronic state. Beams 1 and 2 originating from a single broadband laser source have frequency ω_1 and wave vectors $\mathbf{k}_1$ and $\mathbf{k}_2$, respectively, while beam 3 is a coherent light with frequency ω_3 and wave vector $\mathbf{k}_3$. Due to the nonlinear interaction the Raman vibrational mode will be excited by the beat between beam 1 (beam 2) and beam 3 when $\omega_3-\omega_1$ equals the Raman resonant frequency ω_R. The Raman mode is then probed by beam 2 (beam 1) and the CSRS signal is generated as a result. The frequency and wave vector of the CSRS signal are $\omega_s=2\omega_1-\omega_3$ and $\mathbf{k}_s=\mathbf{k}_1+\mathbf{k}_2-\mathbf{k}_s$, respectively. In the time-delayed CSRS, the signal intensity versus the relative time delay between beams 1 and 2 is studied. We note that the role of beam 1 and beam 2 are interchangeable here. Now, as in the case of RENFWM, CSRS consists of two steps also, that is, the excitation and probing of the Raman mode. However, in the RENFWM beam 2 is used as a excitation beam and beam 1 a probe beam. In contrast, the role of beams 1 and 2 are interchangeable in the CSRS. More specifically, beam 1 (beam 2) is employed as both the excitation and probe beam simultaneously. As a result, the temporal behavior of CSRS is symmetrical about $\tau=0$. This interchangeable feature of beam 1 and beam 2 also makes the second-order coherence function theory failure in the CSRS. Let $u_i(t)$ be the statistical factor that contains the phase and the amplitude fluctuations of the ith beam. Then, it can be shown that the nonlinear polarization responsible for the CSRS is

$$P \propto \int_0^\infty dt' \exp(-\gamma_R t')[u_1(t)u_2(t-t') + u_1(t-t')u_2(t)] . \quad (14)$$

Since beams 1 and 2 come from a single laser source with the relative time delay τ between them, we have $u_1(t)=u(t)$ and $u_2(t)=u(t-\tau)$; therefore

$$P \propto \int_0^\infty dt' \exp(-\gamma_R t')[u(t)u(t-t'-\tau) + u(t-t')u(t-\tau)] . \quad (15)$$

Because $\langle u(t_1)u(t_2)\rangle=0$, it is obvious from Eq. (15) that the absolute square of the stochastic average of the polarization $|\langle P\rangle|^2$ cannot be used to describe the temporal behavior of the CSRS.

In conclusion, we report the first experiment of the time-delayed RENFWM with broadband laser in CS_2. Our results indicate that the temporal behavior of the RENFWM is asymmetric with the maximum of the signal shifted from $\tau=0$. Furthermore, unlike the corresponding CSRS no coherent spike appears at $\tau=0$. From our experimental results the relaxation time of the Raman mode can be extracted directly. We present a second-order coherence function theory to elucidate the physics of the basic features of the time-delayed RENFWM. We also discuss the difference between the RENFWM and CSRS from a physical viewpoint.

ACKNOWLEDGMENTS

The authors gratefully acknowledge the financial support from the Chinese Academy of Sciences, the Chinese National Nature Sciences Foundation, and the Femtosecond Technique & Ultrafast Phenomena Project of China.

[1] N. Morita and T. Yajima, Phys. Rev. A **30**, 2525 (1984).
[2] S. Asaka, H. Nakatsuka, M. Fujiwara, and M. Matsuoka, Phys. Rev. A **29**, 2286 (1984).
[3] H. Nakatsuka, M. Tomita, M. Fujiwara, and S. Asaka, Opt. Commun. **52**, 150 (1984).
[4] R. Beach, D. DeBeer, and S. R. Hartmann, Phys. Rev. A **32**, 3467 (1985).
[5] M. Tomita and M. Matsuoka, J. Opt. Soc. Am. B **3**, 560 (1986).
[6] T. Hattori, A. Terasaki, and T. Kobayashi, Phys. Rev. A **35**, 715 (1987).
[7] P. Fu, Z. Yu, X. Mi, Q. Jiang, and Z. Zhang, Phys. Rev. A **46**, 1530 (1992).
[8] Z. Yu, X. Mi, Q. Jiang, P. Ye, and P. Fu, Opt. Lett. **13**, 117 (1988).
[9] S. K. Saha and R. W. Hellwarth, Phys. Rev. A **27**, 919 (1983).
[10] Z. Yu, H. Lu, P. Ye, and P. Fu, Opt. Commun. **61**, 287 (1987).
[11] J. P. Heritage, Appl. Phys. Lett. **34**, 470 (1979).
[12] Y. R. Shen, *The Principles of Nonlinear Optics* (Wiley, New York, 1984).
[13] P. Fu, Z. Yu, X. Mi, and P. Ye, J. Phys. (Paris) **48**, 2089 (1987).